

# DePT: Decoupled Prompt Tuning

Ji Zhang\*   Shihan Wu\*   Lianli Gao   Hengtao Shen   Jingkuan Song†  
 University of Electronic Science and Technology of China  
 {jizhang.jim, jingkuan.song}@gmail.com

## Abstract

This work breaks through the *Base-New Tradeoff (BNT)* dilemma in prompt tuning, i.e., the better the tuned model generalizes to the base (or target) task, the worse it generalizes to new tasks, and vice versa. Specifically, through an in-depth analysis of the learned features of the base and new tasks, we observe that the BNT stems from a channel bias issue – the vast majority of feature channels are occupied by base-specific knowledge, resulting in the collapse of task-shared knowledge important to new tasks. To address this, we propose the **Decoupled Prompt Tuning (DePT)** framework, which decouples base-specific knowledge from feature channels into an isolated feature space during prompt tuning, so as to maximally preserve task-shared knowledge in the original feature space for achieving better zero-shot generalization on new tasks. Importantly, our DePT is orthogonal to existing prompt tuning methods, hence it can improve all of them. Extensive experiments on 11 datasets show the strong flexibility and effectiveness of DePT. Code: <https://github.com/Koorye/DePT>.

## 1. Introduction

Recent few years have witnessed remarkable progress in large vision-language pre-trained models (VLPMS). One of the striking successes has been achieved by the contrastive language-image pretraining (CLIP) [29] model, which formulates the learning objective as a contrastive loss to learn an alignment between images and their textual descriptions in a common feature space. Despite the ability on capturing open-set visual concepts, the zero-shot generalization performance of VLPMS is greatly reduced when there is a severe *category shift*, *distribution shift* or *domain shift* between the upstream training data and the downstream tasks.

Inspired by the success of prompt engineering in NLP, *prompt tuning* (or *context optimization* [44]) has emerged as a parameter-efficient learning paradigm to transfer knowledge in VLPMS to downstream tasks. Relying on a handful

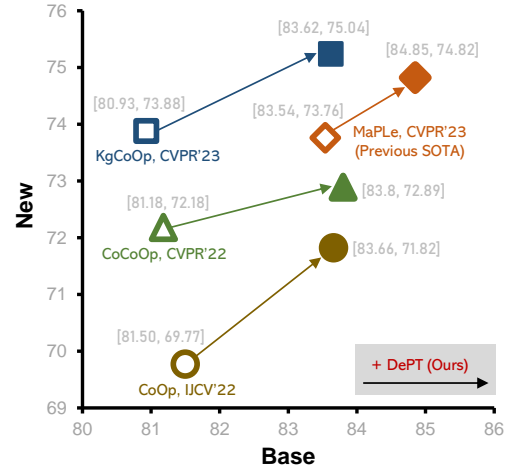


Figure 1. Performance of prompt tuning methods w/ or w/o our DePT framework on base (seen) and new (unseen) tasks. DePT is orthogonal to existing prompt tuning methods, and it can improve the performance on both base and new tasks for all of them. The results are the average on 11 datasets in Table 2.

of training examples, prompt tuning learns a task-specific prompt (i.e., a set of trainable vectors) for each base (a.k.a. target) task, while keeping the weights of VLPMS frozen. Although the advantages are remarkable, existing methods usually fail to escape the *Base-New Tradeoff (BNT)* dilemma, i.e., the better the tuned/adapted model generalizes to the base task, the worse it generalizes to new tasks, and vice versa. Recently, many efforts [37, 43, 45] have been paid to alleviate the performance degradation of the tuned model on new tasks by applying anti-overfitting strategies during prompt tuning. However, the BNT problem is still far from being resolved and its underlying mechanisms are poorly understood over the past years.

In this work, we bridge the gap by proposing **Decoupled Prompt Tuning (DePT)**, a first framework tackling the BNT problem in prompt tuning from a feature decoupling perspective. Concretely, through an in-depth analysis on the feature channels of the base and new tasks learned by the standard Image Text Matching (ITM) head, we observe that the BNT stems from a *channel bias* issue: the vast majority of feature channels are occupied by *base-specific* knowl-

\*Equal contribution.

†Corresponding author.

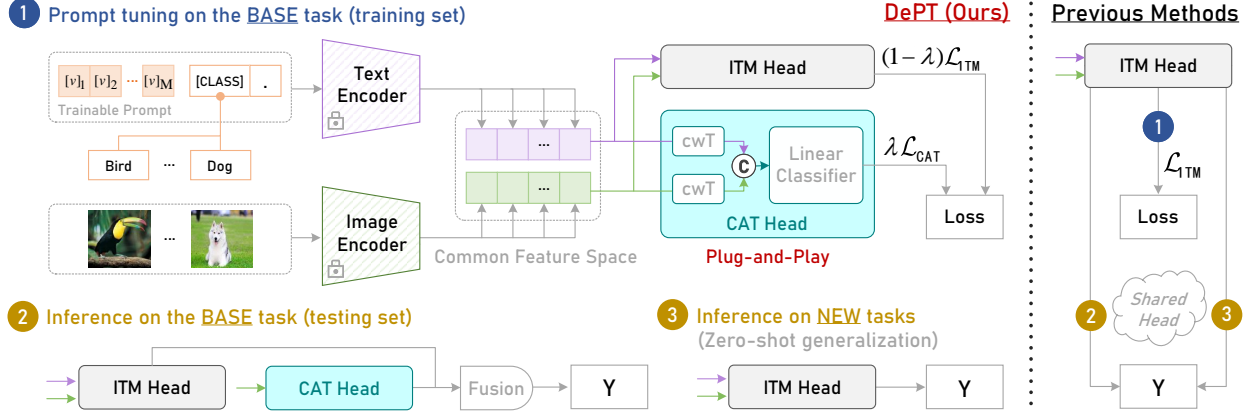


Figure 2. Illustration of our DePT framework (in CoOp [44] style). Unlike previous methods (right) that use the same Image Text Matching (ITM) head for training/inference on the base task and zero-shot generalization on new tasks, our DePT (left) employs a Channel Adjusted Transfer (CAT) head to capture *base-specific* knowledge in an isolated feature space, so as to maximally preserve *task-shared* knowledge in the original feature space for achieving better zero-shot generalization on new tasks. At inference, we further boost the performance on the base task by simply fusing base-specific and task-shared knowledge through the two heads. © denotes the concatenation operation.

edge (i.e., task-specific knowledge of the base task), resulting in the collapse of *task-shared* knowledge important to new tasks (Section 2.2). Inspired by this, we propose to conquer the BNT problem by simultaneously preserving base-specific and task-shared knowledge in feature channels during prompt tuning. To this end, a Channel Adjusted Transfer (CAT) head is devised to capture base-specific knowledge in an isolated feature space, thus facilitating the preservation of task-shared knowledge in the original feature space (Section 2.3). The CAT head is naturally orthogonal to the standard ITM head, hence they can complement each other to circumvent the BNT problem in prompt tuning. Specifically, by performing prompt tuning with the two heads, we establish remarkable zero-shot prediction performance on new tasks through the ITM head, without compromising the results on the base task obtained by the CAT head. Besides, by simply fusing base-specific and task-shared knowledge through the two heads at inference, we boost the performance on the base task significantly (Section 3.2).

**Flexibility and Effectiveness.** Our DePT framework is orthogonal to existing prompt tuning methods, hence it can be flexibly used to overcome the BNT problem for all of them. We evaluate DePT using a broad spectrum of baseline methods, including the *single-modal* prompt tuning methods CoOp [44], CoCoOp [43] and KgCoOp [37], and the *multi-model* prompt tuning method MaPLe [19]. Experimental results on 11 datasets show that DePT consistently improves the performance of those methods, regardless of whether there is a *category shift* (Table 2), *distribution shift* (Table 3) or *domain shift* (Table 4) between base and new tasks, demonstrating the strong flexibility and effectiveness of DePT (Section 3.3). Notably, unlike most previous methods that improve the generalization capability of pretrained models either on base or new tasks, DePT enhances the per-

formance of all those baselines on both base and new tasks – on the four strong baselines, DePT achieves an absolute gain of **1.31%~2.69%** (resp. **0.71%~2.05%**) on base (resp. new) tasks, averaged over 11 datasets (Figure 1).

**Contributions.** Our main contributions are threefold. **1)** We provide an insightful view to analyze the BNT problem in prompt tuning, and for the first time reveal that the BNT stems from the channel bias issue. **2)** We propose the DePT framework to tackle the BNT problem from a feature decoupling perspective, and DePT is orthogonal to existing prompt tuning methods. **3)** We perform experiments on 11 diverse datasets and show that DePT consistently enhances the performance of a broad spectrum of baseline methods<sup>1</sup>.

## 2. Methodology

In this section, we first provide an insightful view to investigate the BNT problem in prompt tuning, then we elaborate on our proposed DePT framework. Before that, we introduce some preliminary concepts.

### 2.1. Preliminaries

**Contrastive Language-Image Pre-training (CLIP) [33].** CLIP targets learning an alignment between image and text features produced by an image encoder and a text encoder, respectively. After seeing 400 million image-text association pairs and performing a contrastive learning paradigm in a common feature space, CLIP captures diverse open-set visual concepts that can readily be generalized to downstream applications. For example, we can achieve zero-shot classification by formulating the classification task as an image-text matching problem. Concretely, we first craft a prompt

<sup>1</sup>We note that our DePT also has the potential to improve *adapter* based task adaptation methods, and we consider it as future work.

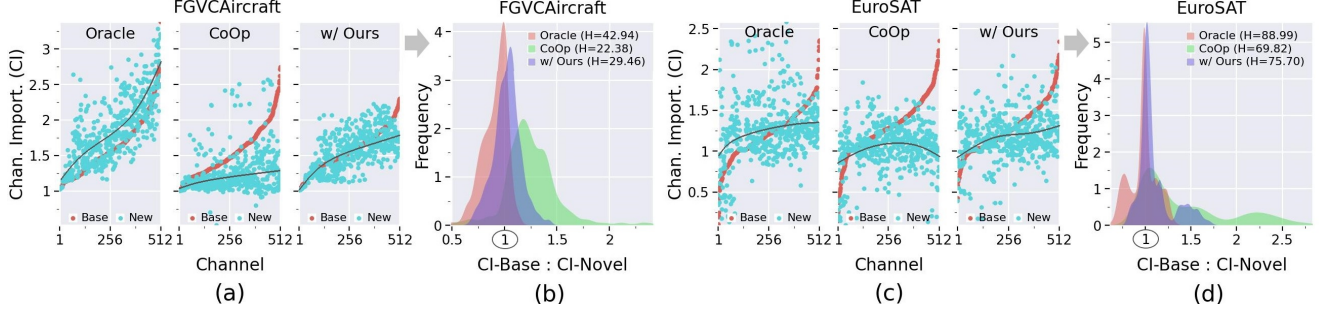


Figure 3. Channel Importance (CI) distributions of base and new tasks learned by the Oracle model and CoOp [44] w/ or w/o our DePT on the datasets FGVCaircraft [25] and EuroSAT [11]. In (a)(c), the indexes of channels in the x-axis are reordered based on the CI of the base task, a point indicates a channel. In (b)(d), the frequency distributions of CI-Base : CI-New are presented, where CI-Base and CI-New are the CI of base and new tasks, respectively; “H” denotes the Harmonic mean [43] of base-task and new-task accuracies.

(e.g., “a photo of a”) to obtain the text features of all inner-task classes, by feeding the class-extended prompt (i.e., “a photo of a [CLASS]”) to the text encoder. Then, we use the image encoder to obtain the image feature of an input example, and predict the class of the example by comparing the cosine distances between the image feature and the text features of classes.

**Prompt Tuning with the Image-Text Matching Head.** Instead of using a hand-crafted prompt (e.g., “a photo of a”), prompt tuning aims to learn a *task-specific* prompt using a handful of training data from the base (or target) task. Let  $[v]_1[v]_2 \dots [v]_l$  denote  $l$  trainable vectors, we forward the class-extended prompt  $c_i = [v]_1[v]_2 \dots [v]_l[\text{CLASS}]$  to the text encoder  $g(\cdot)$  to obtain the text feature of the  $i$ -th class:  $g(c_i)$ . Let  $\mathbf{f}$  denote the image feature of an example  $\mathbf{x}$  obtained by the image encoder, the task-specific prompt can be optimized using a parameter-free Image-Text Matching (ITM) head, which formulates the learning objective as:

$$\mathcal{L}_{\text{ITM}} = - \sum_i \mathbf{y}_i \log \mathcal{P}_{\text{ITM}}(c_i | \mathbf{x}), \quad (1)$$

where  $\mathbf{y}$  is the one-hot label,

$$\mathcal{P}_{\text{ITM}}(c_i | \mathbf{x}) = \frac{\exp(\langle g(c_i), \mathbf{f} \rangle / \tau)}{\sum_{i=1}^M \exp(\langle g(c_i), \mathbf{f} \rangle / \tau)}, \quad (2)$$

$\langle \cdot \rangle$  denotes cosine similarity,  $M$  is the number of classes, and  $\tau$  is the temperature learned by CLIP. During training, the gradients calculated in the ITM head can be back-propagated all the way through the text encoder  $g(\cdot)$  to optimize the trainable vectors in the prompt.

## 2.2. A Closer Look at the BNT Problem

Due to the BNT problem, adapting the pretrained model to the base task  $\mathcal{T}_{\text{base}}$  will decrease the generalization of the model on the new task  $\mathcal{T}_{\text{new}}$ , and vice versa. In this part, provide an insightful view to analyze the BNT problem.

**① Deriving an Oracle Model on  $\mathcal{T}_{\text{base}}$  and  $\mathcal{T}_{\text{new}}$ .** We start the investigation of the BNT problem by deriving an

*oracle* model on  $\mathcal{T}_{\text{base}}$  and  $\mathcal{T}_{\text{new}}$ . Specifically, we adapt the pretrained model to both  $\mathcal{T}_{\text{base}}$  and  $\mathcal{T}_{\text{new}}$  by jointly training the model on the data of the two tasks during prompt tuning. The derived oracle model therefore can be seen as an approximation of a *BNT-free* model, because it does not overfit to either  $\mathcal{T}_{\text{base}}$  or  $\mathcal{T}_{\text{new}}$ . Here, we use the word “oracle”, because the model is derived by leveraging the data of the new task, which is not available in prompt tuning.

**② Calculating Channel Importance for  $\mathcal{T}_{\text{base}}$  or  $\mathcal{T}_{\text{new}}$ .** Denote  $\mathbf{f}_j$  and  $\mathbf{e}_* \in \{\mathbf{e}_i = g(c_i)\}_{i=1}^M$  the  $d$ -dimensional image and text features of the example  $\mathbf{x}_j$  in the learned feature space, respectively. We define the Channel Importance (CI) of the  $r$ -th ( $r = 1, \dots, d$ ) feature channel for the task  $\mathcal{T}_{\text{base}}$  or  $\mathcal{T}_{\text{new}}$  as follows:

$$\text{CI}^{(r)} = \frac{1}{N} \sum_{j=1}^N \frac{\text{ReLU}(\bar{\mathbf{e}}_*^{(r)} \bar{\mathbf{f}}_j^{(r)})}{1/M \sum_{i=1}^M \text{ReLU}(\bar{\mathbf{e}}_i^{(r)} \bar{\mathbf{f}}_j^{(r)}), \quad (3)$$

where  $\bar{\cdot} = \cdot / \|\cdot\|_2$ ,  $N$  is the number of examples in the task. ReLU [1] is used to avoid the denominator being equal to 0. The derived Eq. (3) has an intuitive explanation: a feature channel is of greater importance if it can better distinguish the classes in the task, i.e., the image features are close to the ground-truth text features and far away from the text features of other classes at this channel.

**Analysis.** Based on ① and ②, we wonder what are the differences between the model learned by standard prompt tuning and the derived oracle model w.r.t. the obtained CI distributions of  $\mathcal{T}_{\text{base}}$  and  $\mathcal{T}_{\text{new}}$ . To this end, we take CoOp [44] as the baseline scheme to establish the oracle model using the training data from  $\mathcal{T}_{\text{base}} \cup \mathcal{T}_{\text{new}}$  (see **Sup. Mat.(A)** for details). In Figure 3, we plot the calculated CI distributions of the testing data of  $\mathcal{T}_{\text{base}}$  and  $\mathcal{T}_{\text{new}}$  for CoOp and the oracle model on the datasets FGVCaircraft [25] and EuroSAT [11]. As seen in (a)(c), the CI distributions of base and new tasks obtained by Oracle show greater consistency compared to that by CoOp, which is further confirmed by the results in (b)(d), where the computed values of “CI-Base : CI-New” are close to (resp. larger than) 1.0 in most

cases for Oracle (resp. CoOp). In **(b)(d)**, we also report the Harmonic mean (H) [43] of base-task and new-task accuracies to evaluate the tradeoff. As observed, the oracle model outperforms CoOp considerably, which reveals that most feature channels produced by the oracle model contain *task-shared* knowledge that is valuable for the generalization on both base and new tasks. What’s more, from the results of CoOp in the figure, it is obvious that the achieved CI values of new tasks are significantly lower than that of base tasks at the vast majority of channels. This indicates that most feature channels are occupied by *base-specific* knowledge after prompt tuning, resulting the collapse of task-shared knowledge in the feature channels – we refer this as a *channel bias* issue in this work. Inspired by the above observations, we raise the following question:

*Relying solely on the training data of the base task, can we preserve both base-specific and task-shared knowledge in feature channels to overcome the BNT problem in prompt tuning?*

### 2.3. Decoupled Prompt Tuning

In this work, we answer the above question by proposing Decoupled Prompt Tuning (DePT), a first framework mitigating the BNT problem in prompt tuning from a feature decoupling perspective. An overview of the DePT framework is presented in Figure 2.

**A Plug-and-play Channel Adjusted Transfer Head.** Due to the channel bias issue, striving for base-specific knowledge during prompt tuning will inevitably trigger the catastrophic forgetting of task-shared knowledge in the learned feature channels. To overcome this, our DePT is proposed to decouple base-specific knowledge from feature channels into an isolated feature space, thus facilitating the preservation of task-shared knowledge in the original feature space. To this end, we develop a Channel Adjusted Transfer (CAT) head, which is naturally orthogonal to the standard ITM head (in Section 2.1). Denote  $\mathcal{S}_{\text{img}} = \{\mathbf{f}_j\}_{j=1}^J$  and  $\mathcal{S}_{\text{text}} = \{\mathbf{e}_j\}_{j=1}^J$  the sets of image and text features for a batch of training examples respectively, and  $\mathbf{f}_j, \mathbf{e}_j \in \mathbb{R}^d$ . First, the CAT head leverages a channel-wise Transformation (cwT) layer to transform both  $\mathcal{S}_{\text{img}}$  and  $\mathcal{S}_{\text{text}}$  to a new common feature space. Formally,  $\mathcal{S}'_{\text{img}} = \{\mathbf{f}'_j\}_{j=1}^J$ , and

$$\mathbf{f}'_j = \gamma \odot \mathbf{f}_j + \beta, \quad j = 1, \dots, J, \quad (4)$$

where  $\gamma, \beta \in \mathbb{R}^d$  are trainable scaling and shift vectors. Denote  $\mathcal{S}'_{\text{text}} = \{\mathbf{e}'_j\}_{j=1}^J$  similar to  $\mathcal{S}'_{\text{img}} = \{\mathbf{f}'_j\}_{j=1}^J$ . Next, the CAT head employs a linear classifier to promote the mining of base-specific knowledge using  $\mathcal{S}'_{\text{img}}$  and  $\mathcal{S}'_{\text{text}}$ . Denote  $\mathcal{S}_{\cup} = \mathcal{S}'_{\text{img}} \cup \mathcal{S}'_{\text{text}} = \{\mathbf{s}_j\}_{j=1}^{2J}$  and  $\mathcal{Y}_{\cup} = \{\mathbf{y}_j\}_{j=1}^{2J}$ , where  $\mathbf{y}_j \in \mathbb{R}^M$  is the one-hot label for  $\mathbf{s}_j$ , and  $M$  is the number

of classes of the task. For each pair of  $(\mathbf{s}, \mathbf{y})$ , the CAT head targets minimizing the following cross-entropy loss:

$$\mathcal{L}_{\text{CAT}} = - \sum_i \mathbf{y}_i \log \mathcal{P}_{\text{CAT}}(\mathbf{c}_i | \mathbf{x}), \quad (5)$$

where  $\mathbf{y}$  denotes the one-hot label,

$$\mathcal{P}_{\text{CAT}}(\mathbf{c}_i | \mathbf{x}) = \sigma(\mathbf{W} \cdot \mathbf{s})[i], \quad (6)$$

$\mathbf{W} \in \mathbb{R}^{M \times d}$  denotes the projection matrix for classification,  $\sigma$  denotes the softmax operation. During training, the gradients calculated by  $\mathcal{L}_{\text{CAT}}$  are back-propagated to update the weights in the CAT head (i.e.,  $\gamma, \beta, \mathbf{W}$ ) as well as the trainable prompt (i.e.,  $[\mathbf{v}]_1[\mathbf{v}]_2 \dots [\mathbf{v}]_l$ ). Ablation studies in Section 3.2 show that using two independent cwT layers is more effective than using a shared cwT layer to transform  $\mathcal{S}_{\text{img}}$  and  $\mathcal{S}_{\text{text}}$  to the new feature space.

**Prompt Tuning with Dual Heads.** Instead of solely using the designed CAT head to facilitate the preservation of task-shared knowledge during prompt tuning, our DePT also retains the standard ITM head to learn an alignment of positive image-text pairs in the original feature space, which is of great importance for establishing better zero-shot generalization on new tasks (as proven in Section 3.2). Thus, the overall learning objective of DePT is expressed as:

$$\mathcal{L} = \lambda \mathcal{L}_{\text{CAT}} + (1 - \lambda) \mathcal{L}_{\text{ITM}}, \quad (7)$$

where  $\lambda$  is a balance weight controlling the relative importance of the two loss.

**Test-time Knowledge Fusion for the Base Task.** At inference, the standard ITM head is used to achieve zero-shot generalization/prediction on new tasks in the original feature space. For the base task, our CAT head directly takes the image feature of a testing example as input to predict the in-distribution class label with the linear classifier. Notably, we can further boost the performance on the base task by simply fusing base-specific knowledge in the CAT head as well as task-shared knowledge in the ITM head at inference. According to Eq. (2) and Eq. (6), the prediction probability of the in-distribution testing example  $\mathbf{x}$  belonging to the  $i$ -th class can be computed as:

$$p(\mathbf{c}_i | \mathbf{x}) = \lambda \mathcal{P}_{\text{CAT}}(\mathbf{c}_i | \mathbf{x}) + (1 - \lambda) \mathcal{P}_{\text{ITM}}(\mathbf{c}_i | \mathbf{x}), \quad (8)$$

where the balance weight  $\lambda$  in Eq. (7) is directly used to control the contributions of the two heads for simplification. Pytorch-like pseudocode for the implementation of DePT is presented in **Sup. Mat.(B)**.

## 3. Experiments

In this section, we first present ablation studies to analyze the impacts of different factors on DePT. Next, we validate the flexibility and effectiveness of DePT by applying it to several baseline schemes. We start with an introduction of experimental setup below.



Setting	ITM Head	CAT Head		Test-time fusion for the <i>Base</i> task	Average accuracy over 11 datasets (%)		
		cwT+LC	cwT+ITM		Base	New	H
① ITM only ( <b>Baseline</b> )	✓	✗	✗	✗	81.50	69.77	75.18
② ITM+CAT (CAT=cwT+LC)	✓	✓	✗	✗	82.14 (+0.64)	<b>71.82 (+2.05)</b>	76.63 (+1.45)
v1. Use a shared cwT in CAT	✓	✓	✗	✗	82.24 (+0.74)	70.85 (+1.08)	76.12 (+0.94)
v2. Use an ITM classifier in CAT	✓	✗	✓	✗	82.16 (+0.66)	71.31 (+1.54)	76.35 (+1.17)
v3. Only use image features in CAT	✓	✓	✗	✗	81.11 (-0.39)	70.93 (+1.16)	75.68 (+0.50)
③ ITM+CAT+Fusion ( <b>Our DePT</b> )	✓	✓	✗	✓	<b>83.66 (+2.16)</b>	<b>71.82 (+2.05)</b>	<b>77.29 (+2.11)</b>

Table 1. Ablation study for the designed components of DePT. The baseline method is CoOp [44], and the average accuracy on 11 datasets are reported. The metric “H” indicates the Harmonic-mean [43] of base-task and new-task accuracies. “LC”: Linear Classifier.

### 3.1. Experimental Setup

**Baselines.** We apply our DePT to a broad spectrum of baseline approaches, including the *single-modal* prompt tuning methods CoOp [44], CoCoOp [43], KgCoOp [37] and the *multi-modal* prompt tuning method MaPLe [19]. In particular, by inserting trainable prompts in both the image encoder and text encoder of CLIP, MaPLe yielded state-of-the-art performance. More details of the four baseline methods are available in **Sup. Mat.(C)**.

**Datasets.** We conduct experiments on several datasets from diverse sources. Concretely, for the settings of *base-to-new generalization* and *cross-dataset generalization*, we use **11** datasets: ImgNet [6], Caltech [7], OxfordPets [27], StanfordCars [21], Flowers [26], Food101 [2], FGVC Aircraft [25], EuroSAT [11], UCF101 [32], DTD [5], and SUN397 [36]; for the *domain generalization* setting, we use ImgNet as the source domain (i.e. the base task), and its four variants ImgNet-V2 [31], ImgNet-Sketch [35], ImgNet-A [8] and ImgNet-R [12] as target domains (i.e. new tasks).

**Implementation Details.** Our implementations is based on the open-source repository of MaPLe [19]<sup>2</sup>. For each baseline method, we use the same experimental setup (e.g., feature backbone, prompt lengths and learning rate) as it used in the original implementation. For DePT, the value of  $\lambda$  in Eq. (7)/(8) is set to 0.7; and the learning rate for updating the parameters in the devised CAT head is set to  $6.5 \times \delta$ , where  $\delta$  is the adopted learning rate for prompt tuning by each baseline. For fair comparison, all baselines w/ or w/ our DePT are trained for 10 epochs in our experiments. The above hyperparameters are fixed across all datasets. Unless stated otherwise, the base task is constructed as a many-way 16-shot task. We report base-task and new-task accuracies as well as their harmonic-mean (H) [43] averaged over 3 runs to compare the performance of different methods. All experiments are performed based on NVIDIA V100.

### 3.2. Ablation Studies

Here, we first conduct ablative analysis for DePT in Table 1. Then, we investigate the impact of the balance weight  $\lambda$  on DePT in Figure 4 (Left). Next, we scrutinize the per-

formance of DePT on different training epochs in Figure 4 (Right). Finally, we validate the effectiveness of DePT under different shots (i.e., numbers of training examples per class in base tasks) in Figure 5. We perform experiments using the baseline CoOp [44] in the base-to-new generalization setting, results averaged on the **11** datasets are reported.

**Effectiveness of the Devised Components in DePT.** Our DePT contains two key components, including a plug-and-play CAT head for capturing base-specific knowledge in an isolated feature space, as well as a test-time knowledge fusion strategy for exploring both base-specific and task-shared knowledge to improve the performance on the base task. We conduct component-wise analysis on the two components by progressively adding one of them to the baseline method CoOp [44] in Table 1, where the results are averaged over 11 datasets. From ① and ②, we observe that integrating our CAT head with the standard ITM head for prompt tuning improves both base-task and new-task accuracies of the baseline method, achieving a clear enhancement of the harmonic-mean (by **1.45%**). Notably, ② outperforms ① by up to **2.05%** in terms of new-task accuracy, which demonstrates the effectiveness of our CAT head in facilitating the preservation of task-shared knowledge during prompt tuning. Besides, we also compare the CAT head with its three variants. Concretely, we replace the two independent cwT layers (one for each modality) with a shared cwT layer in v1, we replace the linear classifier with an ITM classifier in v2, and we only feed image features to the liner classifier in v3 (more details are in **Sup. Mat.(D)**). As shown, all the three variants underperform our designed CAT head. What is noteworthy is that directly appending a standard ITM classifier in the cwT-transformed feature space also considerably improves the performance of the baseline on new tasks (see v2), showing the effectiveness of the CAT head for decoupling base-specific and task-shared knowledge during prompt tuning. Besides, we see that using only image features in the CAT head damages the performance on the base task (see v3). This is possibly due to that relying on a limited number of examples for model optimization, the parameters in the CAT head may overfit to the training data of the base task when the gradients of  $\mathcal{L}_{\text{CAT}}$  can not be back-propagated to the text encoder to optimize the parameters of the prompt. What’s more, by simply fusing base-

<sup>2</sup><https://github.com/muzairkhattak/multimodal-prompt-learning>

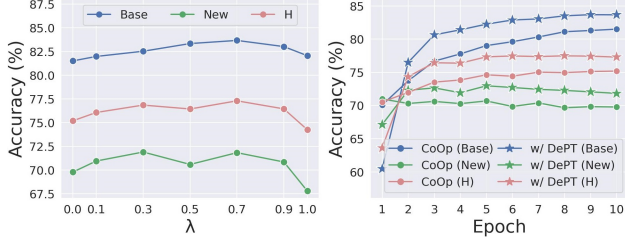


Figure 4. **Left:** Impact of the balance weight  $\lambda$  in Eq. (7)/(8) on DePT. **Right:** Performance of DePT at different training epochs.

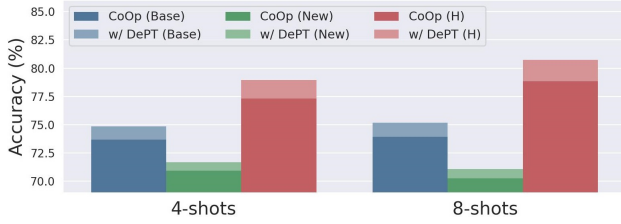


Figure 5. Robustness of DePT under different shots (i.e., numbers of training samples per class in each base task).

specific knowledge in the CAT head and task-shard knowledge in the ITM head at inference, the performance on the base task can be enhanced considerably, achieving an absolute gain of **2.16%** in accuracy compared to the baseline method, as shown in ③.

**Impact of the Balance Weight  $\lambda$  on DePT.** In the proposed DePT, we employ the balance weight  $\lambda$  to control the relative importance of the standard ITM head and our devised CAT head in Eq. (7)/(8). It is necessary to investigate the impact of  $\lambda$  on the performance of DePT. To this end, we set  $\lambda$  to the values of  $\{0.0, 0.1, 0.2, \dots, 1.0\}$ , and report the average testing results on the 11 datasets in Figure 4 (Left). Overall, the performance of DePT gradually increases as the  $\lambda$  value grows from 0.0 to 0.7, after which the performance of DePT gradually decreases and reaches the lowest value when  $\lambda=1.0$ . In particular, when  $\lambda=0.7$  DePT establishes the best performance on both base and new tasks. What is noteworthy is that when  $\lambda=1.0$ , i.e., only our CAT head is used for training, the performance of DePT on new tasks sharply decreases, which suggests that retaining the ITM head to learn an alignment of positive image-text features in the original feature space is of great importance for achieving better zero-shot prediction performance on new tasks.

**Performance of DePT at Different Training Epochs.** In Figure 4 (Right), we report the obtained results of the baseline method w/ or w/o our DePT at different training epochs. As can be observed, our DePT consistently improves the baseline method after epoch 2, in terms of base-task, new-task, and harmonic-mean (H) accuracies. One possible reason for the failure case at epoch 1 is that the weights in the CAL head (i.e.,  $\gamma$ ,  $\beta$ ,  $W$ ) are initialized randomly, thus it is difficult for the CAL head to fully capture base-specific knowledge with only one training epoch. We also see the

baseline method fails to address the BNT problem during prompt tuning – overall, the accuracy of the baseline on new tasks decreases as it’s performance on base tasks increases from epoch 1 to epoch 10. It is obvious that DePT helps the baseline mitigate the BNT problem effectively. Overall, the performance of the baseline method as well as our DePT is saturated at epoch 10.

**Robustness of DePT under Different Shots.** All the aforementioned results are obtained on many-way 16-shot base tasks – for every base task, 16 training examples are sampled from each class for prompt tuning. It is interesting to further scrutinize the robustness of our DePT under different shots. To achieve this, we set the shots to  $\{4, 8, 16\}$ , and report the average testing results of the baseline method w/ or w/o our DePT on the 11 datasets in Figure 5. As can be observed, our DePT consistently improves the baseline method across all 4-shot, 8-shot and 16-shot settings, in terms of base-task, new-task, and harmonic-mean (H) accuracies, showing the robustness of DePT under few shots. In the following section, we follow [19, 37, 43, 44] to evaluate methods in the 16-shot setting. **Sup. Mat.(E)** also presents the performance of DePT on the four baseline approaches for 4-shot and 8-shot settings, where DePT still maintains the advantages as in the 16-shot setting.

### 3.3. Experimental Results

In this part, we apply our DePT to the four baseline approaches, and demonstrate the flexibility and effectiveness of DePT in the following settings: **i)** base-to-new generalization (in Table 2), **ii)** cross-dataset generalization (in Table 3), and **iii)** domain generalization (in Table 4).

**Base-to-New Generalization.** The base-to-new generalization setting evaluates whether the models learned on base tasks can generalize to new tasks with unseen classes, i.e., there is a *category shift* between base and new tasks. For each dataset, we first construct a base task and a new task by equally dividing the dataset into two sets of classes, then we perform prompt tuning on the base task and test the learned model on both the base and new tasks. Table 2 shows the base-to-new generalization performance of the four baselines w/ or w/o DePT on 11 datasets. From the average results, we observe a tradeoff between base-task and new-task accuracies for most of the baseline methods, e.g., Co-CoOp outperforms CoOp on new tasks but underperforms CoOp on base tasks. Notably, DePT consistently improves the performance of all baselines without any performance tradeoffs on base and new tasks. Specifically, DePT improves each baseline in terms of all base-task, new-task and harmonic-mean accuracies. From the results on 11 datasets, we also observe some failure cases, e.g., on the Oxford-Pets dataset, DePT fails to bring clear performance gains on most baseline methods. Possible reasons are as following. **1)** The optimal hyperparameters of DePT for different

Method	Avg over 11 datasets			ImageNet			Caltech101			OxfordPets		
	Base	New	H	Base	New	H	Base	New	H	Base	New	H
CoOp [44]	81.50	69.77	75.18	76.57	69.97	73.12	98.17	<b>94.83</b>	<b>96.47</b>	<b>95.57</b>	97.53	<b>96.54</b>
<b>+DePT</b>	<b>83.66</b>	<b>71.82</b>	<b>77.29</b>	<b>77.13</b>	<b>70.10</b>	<b>73.45</b>	<b>98.33</b>	94.33	96.29	94.70	<b>97.63</b>	96.14
CoCoOp [43]	81.18	72.18	76.42	75.90	<b>70.73</b>	73.23	97.70	93.20	95.40	<b>94.93</b>	<b>97.90</b>	<b>96.39</b>
<b>+DePT</b>	<b>83.80</b>	<b>72.89</b>	<b>77.97</b>	<b>76.87</b>	70.47	<b>73.53</b>	<b>98.37</b>	<b>93.87</b>	<b>96.06</b>	94.03	97.20	95.59
KgCoOp [37]	80.93	73.88	77.25	76.17	<b>70.53</b>	73.24	97.87	94.03	95.91	<b>95.47</b>	<b>97.80</b>	<b>96.62</b>
<b>+DePT</b>	<b>83.62</b>	<b>75.04</b>	<b>79.10</b>	<b>77.03</b>	70.13	<b>73.42</b>	<b>98.30</b>	<b>94.60</b>	<b>96.41</b>	94.33	97.23	95.76
MaPLe [19]	83.54	73.76	78.35	77.23	69.63	73.24	98.30	93.70	95.94	<b>95.17</b>	97.77	<b>96.45</b>
<b>+DePT</b>	<b>84.85</b>	<b>74.82</b>	<b>79.52</b>	<b>77.87</b>	<b>70.23</b>	<b>73.85</b>	<b>98.53</b>	<b>95.03</b>	<b>96.75</b>	95.03	<b>97.83</b>	96.41
Method	StanfordCars			Flowers102			Food101			FGVCAircraft		
	Base	New	H	Base	New	H	Base	New	H	Base	New	H
CoOp [44]	74.30	72.10	73.18	97.07	<b>74.33</b>	<b>84.19</b>	90.43	90.97	90.70	31.70	17.30	22.38
<b>+DePT</b>	<b>79.67</b>	<b>72.40</b>	<b>75.86</b>	<b>98.20</b>	72.00	83.08	<b>90.43</b>	<b>91.33</b>	<b>90.88</b>	<b>42.53</b>	<b>22.53</b>	<b>29.46</b>
CoCoOp [43]	70.77	72.50	71.62	95.03	69.07	80.00	<b>90.57</b>	91.20	<b>90.88</b>	35.63	<b>32.70</b>	34.10
<b>+DePT</b>	<b>79.87</b>	<b>73.33</b>	<b>76.46</b>	<b>98.33</b>	<b>72.57</b>	<b>83.51</b>	90.30	<b>91.30</b>	90.80	<b>43.07</b>	31.30	<b>36.25</b>
KgCoOp [37]	71.13	74.67	72.86	95.90	74.83	84.07	90.47	<b>91.60</b>	91.03	35.10	<b>35.20</b>	35.15
<b>+DePT</b>	<b>79.13</b>	<b>75.47</b>	<b>77.26</b>	<b>98.00</b>	<b>76.37</b>	<b>85.84</b>	<b>90.50</b>	<b>91.60</b>	<b>91.05</b>	<b>43.20</b>	34.83	<b>38.57</b>
MaPLe [19]	76.30	<b>72.53</b>	74.37	97.23	72.07	82.78	90.30	<b>91.53</b>	90.91	40.57	<b>36.47</b>	<b>38.31</b>
<b>+DePT</b>	<b>80.93</b>	71.73	<b>76.06</b>	<b>98.03</b>	<b>73.17</b>	<b>83.79</b>	<b>90.33</b>	<b>91.53</b>	<b>90.93</b>	<b>44.53</b>	32.80	37.78
Method	SUN397			DTD			EuroSAT			UCF101		
	Base	New	H	Base	New	H	Base	New	H	Base	New	H
CoOp [44]	81.13	<b>76.07</b>	78.52	79.33	49.70	61.11	<b>89.35</b>	57.30	69.82	83.87	69.80	76.19
<b>+DePT</b>	<b>82.37</b>	75.07	<b>78.55</b>	<b>83.20</b>	<b>56.13</b>	<b>67.04</b>	88.27	<b>66.27</b>	<b>75.70</b>	<b>85.43</b>	<b>72.17</b>	<b>78.24</b>
CoCoOp [43]	79.50	76.27	77.85	77.37	52.97	62.88	87.97	63.63	73.85	82.33	72.40	77.05
<b>+DePT</b>	<b>82.20</b>	<b>76.73</b>	<b>79.37</b>	<b>82.77</b>	<b>55.40</b>	<b>66.37</b>	<b>90.27</b>	<b>66.87</b>	<b>76.82</b>	<b>85.70</b>	<b>72.80</b>	<b>78.73</b>
KgCoOp [37]	80.40	77.30	78.82	78.27	57.93	66.58	85.77	63.40	72.91	83.73	75.40	79.35
<b>+DePT</b>	<b>82.33</b>	<b>77.80</b>	<b>80.00</b>	<b>82.20</b>	<b>59.13</b>	<b>68.78</b>	<b>89.03</b>	<b>71.07</b>	<b>79.04</b>	<b>85.80</b>	<b>77.23</b>	<b>81.29</b>
MaPLe [19]	81.93	<b>76.50</b>	79.12	81.93	58.20	68.06	<b>94.67</b>	66.73	78.28	85.30	76.23	80.51
<b>+DePT</b>	<b>82.90</b>	76.40	<b>79.52</b>	<b>83.87</b>	<b>59.93</b>	<b>69.91</b>	94.43	<b>76.23</b>	<b>84.36</b>	<b>86.87</b>	<b>78.10</b>	<b>82.25</b>

Table 2. Base-to-new generalization performance of four baselines w/ or w/o our DePT on 11 datasets.

Method	Source	Target										
	ImgNet	Caltech101	OxfordPets	StanfordCars	Flowers102	Food101	FGVCAircraft	SUN397	DTD	EuroSAT	UCF101	Avg
CoOp [44]	71.80	<b>93.97</b>	89.60	64.60	69.13	85.47	20.70	65.70	43.07	44.50	67.23	64.40
<b>+DePT</b>	<b>72.63</b>	93.30	<b>90.00</b>	<b>65.53</b>	<b>70.50</b>	<b>85.97</b>	<b>21.90</b>	<b>66.07</b>	<b>43.17</b>	<b>44.97</b>	<b>68.80</b>	<b>65.02</b>
CoCoOp [43]	71.17	<b>94.30</b>	<b>90.80</b>	65.53	71.80	86.13	22.83	<b>67.73</b>	<b>45.57</b>	43.47	69.10	65.73
<b>+DePT</b>	<b>72.77</b>	94.10	90.63	<b>66.23</b>	<b>72.17</b>	<b>86.27</b>	<b>22.90</b>	67.30	45.50	<b>44.17</b>	<b>69.53</b>	<b>65.88</b>
KgCoOp [37]	71.17	94.17	89.70	64.77	70.30	<b>86.47</b>	22.43	<b>66.83</b>	44.43	<b>43.53</b>	68.00	65.06
<b>+DePT</b>	<b>72.77</b>	<b>94.23</b>	<b>90.03</b>	<b>65.57</b>	<b>70.57</b>	86.37	<b>23.27</b>	66.67	<b>45.97</b>	<b>43.53</b>	<b>69.30</b>	<b>65.55</b>
MaPLe [19]	72.47	<b>92.97</b>	<b>90.20</b>	63.97	70.03	84.83	23.23	66.00	43.23	40.03	67.23	64.17
<b>+DePT</b>	<b>73.27</b>	92.53	90.10	<b>64.60</b>	<b>70.10</b>	<b>85.57</b>	<b>23.63</b>	<b>66.40</b>	<b>45.03</b>	<b>40.13</b>	<b>67.53</b>	<b>64.56</b>

Table 3. Cross-dataset generalization performance of four baselines w/ or w/o our DePT on 11 datasets.

Method	Source	Target			
	ImgNet	ImgNet-V2	ImgNet-Sk.	ImgNet-R	ImgNet-A
CoOp [44]	70.53	64.13	49.13	77.20	51.43
<b>+DePT</b>	<b>70.70</b>	<b>64.13</b>	<b>49.40</b>	<b>77.33</b>	<b>51.57</b>
CoCoOp [43]	<b>70.70</b>	63.93	48.93	<b>76.97</b>	50.87
<b>+DePT</b>	70.57	<b>63.97</b>	<b>49.83</b>	76.87	<b>50.90</b>
KgCoOp [37]	70.33	63.47	48.77	<b>76.73</b>	50.53
<b>+DePT</b>	<b>70.63</b>	<b>63.70</b>	<b>48.90</b>	76.57	<b>50.77</b>
MaPLe [19]	70.87	63.87	49.00	77.03	49.03
<b>+DePT</b>	<b>70.97</b>	<b>64.33</b>	<b>49.33</b>	<b>77.37</b>	<b>49.70</b>

Table 4. Domain generalization performance of four baselines w/ or w/o our DePT on the ImgNet dataset.

datasets and baselines are quite different, while we fix them across all datasets and baselines. 2) When the *category shift* between downstream tasks and the upstream data for model (i.e. CLIP) pretraining is too small, the advantages of our DePT as well as prompt tuning for task adaptation become less significant.

**Cross-Dataset Generalization.** The cross-dataset generalization setting evaluates whether the model learned on the source dataset can generalize to unseen target datasets, i.e., there is a *distribution shift* between base and new tasks. In this experiment, we follow the baselines to regard ImgNet as the source dataset and other 10 datasets as target datasets. Table 3 presents the performance of the four baselines w/ or w/o our DePT on the 11 datasets. As can be seen, our DePT consistently improves the accuracy on the source dataset for all baselines, without compromising the performance on 10 target datasets in most cases. Notably, on average our DePT consistently enhances the performance of all baselines on both the source and target datasets, suggesting DePT is robust to the distribution shift. Moreover, we see that MaPLe establishes the best performance among the four baseline methods in Table 2, but its performance is inferior to CoCoOp and KgCoOp in Table 3. This is probably due to the

task-shared knowledge learned by MaPLe is not generalizable enough under distribution shift.

**Domain Generalization.** The domain generalization setting evaluates whether the model learned on the source domain can generalize to unseen domains, i.e., there is a *domain shift* between base and new tasks. Following the baselines, we regard the ImgNet dataset as the source domain and other four ImgNet variants as target domains. Table 4 presents the domain generalization performance of the four baselines w/ or w/o our DePT. As seen, DePT still maintains the advantages as in previous experiments. Specifically, our DePT consistently improves the accuracy on the source domain without compromising the performance on the target domains in most cases for all baselines, which reveals that the models learned with DePT are more domain-generalizable. Moreover, we see that the performance gains achieved by DePT in Table 4 are not as significant as that achieved in Tables 2 and 3. Possible reasons are twofold. 1) The domain generalization setting is more challenging compared to the base-to-new/cross-dataset generalization setting, as shown in prior works [37, 43, 45]. 2) It is difficult for DePT to simultaneously capture task-shared and domain-agnostic knowledge without accessing the data of target domains during prompt tuning.

## 4. Related Work

**Vision-Language Pre-training.** By establishing a connection between images and natural language from countless image-text pairs, large vision-language pre-trained models (VLPMS) have shown strong zero-shot generalization on various downstream tasks. Generally, VLPMS leverage three types of pre-text tasks for modeling the semantic correspondence between the vision and language modalities, including 1) image-text matching [17, 20], 2) contrastive learning [16, 22], and 3) masked vision/language prediction [20, 23]. In this work, we mainly focus on VLPMS establishing image-text alignment with contrastive learning, motivated by their excellent generalization ability to downstream tasks. For example, after seeing 400 million text-image pairs, CLIP [29] learns an alignment between visual and textual features output by a image encoder and a text encoder respectively. Beyond recognition [19, 41, 43], CLIP also show great potential for other downstream applications, such as image manipulation [28, 33], video-text retrieval [4, 24], and dense prediction [30, 42].

**Task Adaptation on VLPMS.** The remarkable success of VLPMS have brought new light but also pose a new question: how to efficiently adapt the knowledge from VLPMS to different downstream tasks? The most direct solution is *full-finetuning*, which fixes the architecture of VLPMS and tunes all the parameters on the target task. While the results are impressive, this line of work becomes prohibitively

expensive with the ever-increasing size of parameters of VLPMS. To remedy this, *partial-finetuning* has been proposed to update only a small number of extra parameters (a.k.a. *adapters*) while keeping most pre-trained parameters frozen. Representative approaches are Adapters [13], CLIP-Adapter [9], LoRA [14], BitFit [38] and Diff-pruning [10].

**Prompt Tuning.** Inspired from the field of NLP, a rich line of recent works adapts VLPMS to downstream tasks by learning task-specific prompts in an end-to-end manner [3, 34, 45]. Since only a handful of labeled examples are available during training, prompt tuning can be regarded as few-shot learning task [39, 40]. In particular, CoOp [44] performs task adaptation by optimizing a set of prompt vectors at the language branch of CLIP. While simple and effective, CoOp tends to achieve poor generalization on new tasks after overfitting to the base (or target) task. To overcome this issue, CoCoOp [43] learns a lightweight meta-net to generate an input-conditional token for each input image. By reducing the discrepancy between the hand-crafted prompt and the trainable prompt tokens, KgCoOp [43] significantly improves the generalization of the adapted models on new tasks. Similarly, ProGrad [45] mitigates the overfitting issue by regularizing each tuning step that is not to conflict with the general knowledge of the hand-crafted prompt. Unlike the aforementioned methods that mainly focus on developing efficient textual prompts, a rich line of works also explores visual prompts for task adaptation [15, 18]. In the recent work [19], authors propose the first multi-model prompt tuning method MaPLe [19]. By adding trainable prompts at both the language and text branches of CLIP, MaPLe yields remarkable performance on both the base task and new tasks. In this work, we propose DePT to tackle the base-new tradeoff problem in prompt tuning. More importantly, DePT is orthogonal to existing prompt tuning methods, hence it can improve all of them.

## 5. Conclusions

This work proposes Decoupled Prompt Tuning (DePT), a novel framework tackling the Base-New Tradeoff (BNT) problem in prompt tuning from a feature decoupling perspective. First, we provide an insightful view to analyze the BNT problem, and for the first time reveal that the BNT stems from the channel bias issue. Second, we present the DePT framework for tackling the BNT problem, and DePT is orthogonal to existing prompt tuning methods. Finally, we apply our DePT to a broad spectrum of baseline methods, and the obtained experimental results on 11 datasets validate the flexibility and effectiveness of DePT. We hope this work can bring some inspiration to prompt tuning and other related fields. To facilitate future research, we have made our code and pretrained models publicly available at: <https://github.com/Koorye/DePT>.



## References

- [1] Abien Fred Agarap. Deep learning using rectified linear units (relu). *arXiv preprint arXiv:1803.08375*, 2018. [3](#)
- [2] Lukas Bossard, Matthieu Guillaumin, and Luc Van Gool. Food-101—mining discriminative components with random forests. In *ECCV*, pages 446–461. Springer, 2014. [5](#)
- [3] Guangyi Chen, Weiran Yao, Xiangchen Song, Xinyue Li, Yongming Rao, and Kun Zhang. Prompt learning with optimal transport for vision-language models. *ICLR*, 2022. [8](#)
- [4] Xing Cheng, Hezheng Lin, Xiangyu Wu, Fan Yang, and Dong Shen. Improving video-text retrieval by multi-stream corpus alignment and dual softmax loss. *arXiv preprint arXiv:2109.04290*, 2021. [8](#)
- [5] Mircea Cimpoi, Subhansu Maji, Iasonas Kokkinos, Sammy Mohamed, and Andrea Vedaldi. Describing textures in the wild. In *CVPR*, pages 3606–3613, 2014. [5](#)
- [6] Jia Deng, Wei Dong, Richard Socher, Li-Jia Li, Kai Li, and Li Fei-Fei. Imagenet: A large-scale hierarchical image database. In *CVPR*, pages 248–255. Ieee, 2009. [5](#)
- [7] Li Fei-Fei, Rob Fergus, and Pietro Perona. Learning generative visual models from few training examples: An incremental bayesian approach tested on 101 object categories. In *CVPRW*, pages 178–178. IEEE, 2004. [5](#)
- [8] Haoran Gao, Hua Zhang, Xingguo Yang, Wenmin Li, Fei Gao, and Qiaoyan Wen. Generating natural adversarial examples with universal perturbations for text classification. *Neurocomputing*, 471:175–182, 2022. [5](#)
- [9] Peng Gao, Shijie Geng, Renrui Zhang, Teli Ma, Rongyao Fang, Yongfeng Zhang, Hongsheng Li, and Yu Qiao. Clip-adapter: Better vision-language models with feature adapters. *arXiv preprint arXiv:2110.04544*, 2021. [8](#)
- [10] Demi Guo, Alexander M Rush, and Yoon Kim. Parameter-efficient transfer learning with diff pruning. *ACL*, 2020. [8](#)
- [11] Patrick Helber, Benjamin Bischke, Andreas Dengel, and Damian Borth. Eurosat: A novel dataset and deep learning benchmark for land use and land cover classification. *IEEE Journal of Selected Topics in Applied Earth Observations and Remote Sensing*, 12(7):2217–2226, 2019. [3](#), [5](#), [11](#)
- [12] Dan Hendrycks, Steven Basart, Norman Mu, Saurav Kadavath, Frank Wang, Evan Dorundo, Rahul Desai, Tyler Zhu, Samyak Parajuli, Mike Guo, et al. The many faces of robustness: A critical analysis of out-of-distribution generalization. In *ICCV*, pages 8340–8349, 2021. [5](#)
- [13] Neil Houlsby, Andrei Giurgiu, Stanislaw Jastrzebski, Bruna Morrone, Quentin De Laroussilhe, Andrea Gesmundo, Mona Attariyan, and Sylvain Gelly. Parameter-efficient transfer learning for nlp. In *ICML*, pages 2790–2799, 2019. [8](#)
- [14] Edward J Hu, Yelong Shen, Phillip Wallis, Zeyuan Allen-Zhu, Yuanzhi Li, Shean Wang, Lu Wang, and Weizhu Chen. Lora: Low-rank adaptation of large language models. *arXiv preprint arXiv:2106.09685*, 2021. [8](#)
- [15] Qidong Huang, Xiaoyi Dong, Dongdong Chen, Weiming Zhang, Feifei Wang, Gang Hua, and Nenghai Yu. Diversity-aware meta visual prompting. In *CVPR*, pages 10878–10887, 2023. [8](#)
- [16] Yuqi Huo, Manli Zhang, Guangzhen Liu, Haoyu Lu, Yizhao Gao, Guoxing Yang, Jingyuan Wen, Heng Zhang, Baogui Xu, Weihao Zheng, et al. Wenlan: Bridging vision and language by large-scale multi-modal pre-training. *arXiv preprint arXiv:2103.06561*, 2021. [8](#)
- [17] Chao Jia, Yinfei Yang, Ye Xia, Yi-Ting Chen, Zarana Parekh, Hieu Pham, Quoc Le, Yun-Hsuan Sung, Zhen Li, and Tom Duerig. Scaling up visual and vision-language representation learning with noisy text supervision. In *ICML*, pages 4904–4916, 2021. [8](#)
- [18] Menglin Jia, Luming Tang, Bor-Chun Chen, Claire Cardie, Serge Belongie, Bharath Hariharan, and Ser-Nam Lim. Visual prompt tuning. In *ECCV*, pages 709–727, 2022. [8](#)
- [19] Muhammad Uzair Khattak, Hanoona Rasheed, Muhammad Maaz, Salman Khan, and Fahad Shahbaz Khan. Maple: Multi-modal prompt learning. In *CVPR*, pages 19113–19122, 2023. [2](#), [5](#), [6](#), [7](#), [8](#), [12](#), [13](#)
- [20] Wonjae Kim, Bokyoung Son, and Ildoo Kim. Vilt: Vision-and-language transformer without convolution or region supervision. In *International Conference on Machine Learning*, pages 5583–5594. PMLR, 2021. [8](#)
- [21] Jonathan Krause, Michael Stark, Jia Deng, and Li Fei-Fei. 3d object representations for fine-grained categorization. In *ICCVW*, pages 554–561, 2013. [5](#)
- [22] Junnan Li, Ramprasaath Selvaraju, Akhilesh Gotmare, Shafiq Joty, Caiming Xiong, and Steven Chu Hong Hoi. Align before fuse: Vision and language representation learning with momentum distillation. *NeurIPS*, 34:9694–9705, 2021. [8](#)
- [23] Jiasen Lu, Dhruv Batra, Devi Parikh, and Stefan Lee. Vilbert: Pretraining task-agnostic visiolinguistic representations for vision-and-language tasks. *NeurIPS*, 32, 2019. [8](#)
- [24] Yiwei Ma, Guohai Xu, Xiaoshuai Sun, Ming Yan, Ji Zhang, and Rongrong Ji. X-clip: End-to-end multi-grained contrastive learning for video-text retrieval. In *ACM MM*, pages 638–647, 2022. [8](#)
- [25] Subhansu Maji, Esa Rahtu, Juho Kannala, Matthew Blaschko, and Andrea Vedaldi. Fine-grained visual classification of aircraft. *arXiv preprint arXiv:1306.5151*, 2013. [3](#), [5](#), [11](#)
- [26] Maria-Elena Nilsback and Andrew Zisserman. Automated flower classification over a large number of classes. In *ICVGIP*, pages 722–729. IEEE, 2008. [5](#)
- [27] Omkar M Parkhi, Andrea Vedaldi, Andrew Zisserman, and CV Jawahar. Cats and dogs. In *CVPR*, pages 3498–3505. IEEE, 2012. [5](#)
- [28] Or Patashnik, Zongze Wu, Eli Shechtman, Daniel Cohen-Or, and Dani Lischinski. Styleclip: Text-driven manipulation of stylegan imagery. In *CVPR*, pages 2085–2094, 2021. [8](#)
- [29] Alec Radford, Jong Wook Kim, Chris Hallacy, Aditya Ramesh, Gabriel Goh, Sandhini Agarwal, Girish Sastry, Amanda Askell, Pamela Mishkin, Jack Clark, et al. Learning transferable visual models from natural language supervision. In *ICML*, pages 8748–8763, 2021. [1](#), [8](#)
- [30] Yongming Rao, Wenliang Zhao, Guangyi Chen, Yansong Tang, Zheng Zhu, Guan Huang, Jie Zhou, and Jiwen Lu. Denseclip: Language-guided dense prediction with context-aware prompting. In *CVPR*, pages 18082–18091, 2022. [8](#)

- [31] Benjamin Recht, Rebecca Roelofs, Ludwig Schmidt, and Vaishaal Shankar. Do imagenet classifiers generalize to imagenet? In *ICML*, pages 5389–5400. PMLR, 2019. 5
- [32] Khurram Soomro, Amir Roshan Zamir, and Mubarak Shah. Ucf101: A dataset of 101 human actions classes from videos in the wild. *arXiv preprint arXiv:1212.0402*, 2012. 5
- [33] Can Wang, Menglei Chai, Mingming He, Dongdong Chen, and Jing Liao. Clip-nerf: Text-and-image driven manipulation of neural radiance fields. In *CVPR*, pages 3835–3844, 2022. 2, 8
- [34] Feng Wang, Manling Li, Xudong Lin, Hairong Lv, Alexander G Schwing, and Heng Ji. Learning to decompose visual features with latent textual prompts. *ICLR*, 2022. 8
- [35] Haoan Wang, Songwei Ge, Zachary Lipton, and Eric P Xing. Learning robust global representations by penalizing local predictive power. *NeurIPS*, 32, 2019. 5
- [36] Jianxiong Xiao, James Hays, Krista A Ehinger, Aude Oliva, and Antonio Torralba. Sun database: Large-scale scene recognition from abbey to zoo. In *CVPR*, pages 3485–3492. IEEE, 2010. 5
- [37] Hantao Yao, Rui Zhang, and Changsheng Xu. Visual-language prompt tuning with knowledge-guided context optimization. In *CVPR*, pages 6757–6767, 2023. 1, 2, 5, 6, 7, 8, 12, 13
- [38] Elad Ben Zaken, Shauli Ravfogel, and Yoav Goldberg. Bitfit: Simple parameter-efficient fine-tuning for transformer-based masked language-models. *arXiv preprint arXiv:2106.10199*, 2021. 8
- [39] Ji Zhang, Lianli Gao, Xu Luo, Hengtao Shen, and Jingkuan Song. Deta: Denoised task adaptation for few-shot learning. *arXiv preprint arXiv:2303.06315*, 2023. 8
- [40] Ji Zhang, Jingkuan Song, Lianli Gao, and Hengtao Shen. Free-lunch for cross-domain few-shot learning: Style-aware episodic training with robust contrastive learning. In *ACM MM*, pages 2586–2594, 2022. 8
- [41] Renrui Zhang, Wei Zhang, Rongyao Fang, Peng Gao, Kunchang Li, Jifeng Dai, Yu Qiao, and Hongsheng Li. Tip-adapter: Training-free adaption of clip for few-shot classification. In *ECCV*, pages 493–510. Springer, 2022. 8
- [42] Chong Zhou, Chen Change Loy, and Bo Dai. Extract free dense labels from clip. In *ECCV*, pages 696–712. Springer, 2022. 8
- [43] Kaiyang Zhou, Jingkang Yang, Chen Change Loy, and Ziwei Liu. Conditional prompt learning for vision-language models. In *CVPR*, pages 16816–16825, 2022. 1, 2, 3, 4, 5, 6, 7, 8, 12, 13
- [44] Kaiyang Zhou, Jingkang Yang, Chen Change Loy, and Ziwei Liu. Learning to prompt for vision-language models. *International Journal of Computer Vision*, 130(9):2337–2348, 2022. 1, 2, 3, 5, 6, 7, 8, 11, 12, 13
- [45] Beier Zhu, Yulei Niu, Yucheng Han, Yue Wu, and Hanwang Zhang. Prompt-aligned gradient for prompt tuning. *ICCV*, 2023. 1, 8

## Supplementary Material

### A. Details of the Oracle Model

In this work, we start the investigation of the BNT problem in prompt tuning by deriving an *oracle* model on  $\mathcal{T}_{\text{base}}$  and  $\mathcal{T}_{\text{new}}$ . More specifically, we adapt the pretrained model to both  $\mathcal{T}_{\text{base}}$  and  $\mathcal{T}_{\text{new}}$  by jointly training the model on the data of the two tasks during prompt tuning. We achieve this with the following steps.

**Step-1.** We follow the base-to-new generalization setting to construct the base task  $\mathcal{T}_{\text{base}}$  and the new task  $\mathcal{T}_{\text{new}}$  by equally dividing the dataset FGVC Aircraft [25] or EuroSAT [11] into two sets of classes.

**Step-2.** We construct the training set  $\mathcal{S}$  by sampling 16 training examples from each class of the base and new tasks on the dataset FGVC Aircraft [25] or EuroSAT [11].

**Step-3.** We use CoOp [44] as the baseline method to perform prompt tuning on  $\mathcal{S}$  to obtain the oracle model.

The derived oracle model therefore can be seen as an approximation of a *BNT-free* model, because it does not overfit to either  $\mathcal{T}_{\text{base}}$  or  $\mathcal{T}_{\text{new}}$ . At inference, the *in-distribution* testing data from  $\mathcal{T}_{\text{base}}$  and *out-of-distribution* testing data from  $\mathcal{T}_{\text{new}}$  are used to evaluate the derived oracle model.

### B. Details of the Implementation of DePT.

In this work, we propose the DePT framework to tackle the BNT problem in prompt tuning from a feature decoupling perspective.

**During training,** our DePT jointly leverages the standard Image-Text Matching (ITM) head (w/ the  $\mathcal{L}_{\text{ITM}}$  loss) together with our devised Channel Adjusted Transfer (CAT) head (w/ the  $\mathcal{L}_{\text{CAT}}$  loss) to encourage base-specific and task-shared knowledge in the original and transformed feature spaces respectively, so as to establish better generalization performance on both base and new tasks.

**At inference,** the ITM head is used for zero-shot generalization on new tasks with unseen classes, and the CAL head can directly take the image feature of a testing image as input to predict the in-distribution class label for the base task. Notably, we further boost the performance on the base task by simply fusing base-specific knowledge in the CAL head as well as task-shared knowledge in the ITM head.

We present the Pytorch-like pseudocode for the core of an implementation of the proposed DePT framework in Figure 6, where all the trainable parameters in the CAT head are initialized randomly. Our DePT can be performed based on a single NVIDIA A100. Notably, DePT is orthogonal to existing prompt tuning methods, hence it can be used as a plugin to improve all of them. More details are available at:

<https://github.com/Koorye/DePT>

```
# X[n, h, w, c]: minibatch of aligned images
# E[m, r]: r-dimensional word embeddings of m classes
# cwt_I(): cwt layer for transforming image features
# cwt_T(): cwt layer for transforming text features
# lc(): linear classifier
# Lamb: balance weight
# L[n, m]: one-hot labels of the images, m is the num of classes

### TRAINING
# obtain image and text features of the minibatch
F_I = image_encoder(X) # [n, d]
F_T = text_encoder(E) # [c, d]

# compute the ITM loss using original image and text features
logit_sim = cal_ITM_similarity(F_I, F_T)
L_ITM = cross_entropy(logit_sim, L)

# compute the CAT loss using transformed image and text features
F_I, F_T = cwt_I(F_I), cwt_T(F_T)
logit_linear = lc(torch.cat([F_I, F_T[L]]))
L_CAT = cross_entropy(logit_linear, torch.cat([L, L]))

# combine L_ITM with L_CAT to update the trainable parameters
L = Lamb * L_CAT + (1 - Lamb) * L_ITM

### INFERENCE
# obtain the text features of all m inner-task classes
F_T = text_encoder(E) # [m, d]

# obtain the image feature of the an input image x[1, h, w, c]
f = image_encoder(x) # [1, d]

# obtain the ITM logits of the image
logit_sim = cal_ITM_similarity(f, F_T)

# CASE-1: x is from new tasks
Y <- logit_sim

# CASE-2: x is from the base task
logit_linear = lc(cwt_I(f))
Y <- Lamb * logit_linear + (1 - Lamb) * logit_sim
```

Figure 6. Pytorch-like pseudocode for the implementation of our DePT framework, consisting of TRAINING/INFERENCE on the base task as well as zero-shot INFERENCE on new tasks with out-of-distribution classes.

### C. Details of the Baseline Methods

In our experiments, we apply our DePT to four diverse baseline approaches to demonstrate the flexibility and effectiveness of DePT. Here, we elaborate on the four diverse baseline methods. Qualitative comparison of the those baseline methods are illustrated in Table 5.

**CoOp [44]<sup>3</sup>.** Context Optimization (CoOp) is a simple yet efficient prompt tuning method specifically for adapting CLIP-like vision-language pre-trained models (VLPs) to downstream tasks. Instead of using a *hand-crafted* prompt (e.g. “a photo of a”), the goal in CoOp is to learn a *soft* prompt (modeled as trainable embedding vectors) during training, while the entire pretrained weights are kept fixed. Besides, the prompt is only used at the text encoder branch of the CLIP model for CoOp.

<sup>3</sup><https://github.com/KaiyangZhou/CoOp>

Method	Prompt Type	Branch	Location
CoOp [44]	Soft	Text Encoder	Word Embed.
CoCoOp [43]	Soft (dynamic)	Text Encoder	Word Embed.
KgCoOp [37]	Soft & Hand-craft	Text Encoder	Word Embed.
MaPLe [19]	Soft	Image & Text Encoder	Deep Features

Table 5. Comparison of the four diverse baseline methods.

**CoCoOp [43]**<sup>4</sup>. As an extension of CoOp, the goal of Conditional Context Optimization (CoCoOp) is to alleviate the overfitting issue of CoOp, i.e., the learned context by CoOp is not generalizable to wider unseen classes/tasks within the same dataset. To this end, CoCoOp extends CoOp by further learning a lightweight meta-net to generate for each image an input-conditional embedding vectors. Unlike CoOp that uses a static prompt for each task during training, CoCoOp uses *dynamic* prompts to adapt the pretrained model to instances and is thus less sensitive to category shift.

**KgCoOp [37]**<sup>4</sup>. The recently proposed Knowledge-guided Context Optimization (KgCoOp) also focuses on tackling the overfitting issue of CoOp. Particularly, KgCoOp employs the *hand-crafted* prompt (i.e. “a photo of a”) to guide the learning of the soft prompt during training. Moreover, authors in [37] reveal that the larger the distance between textual embeddings generated by the soft prompt and the hand-crafted prompt, the more severe the performance degradation on new tasks.

**MaPLe [19]**<sup>5</sup>. Multi-modal Prompt Learning (MaPLe) for the first time integrates training prompts in both vision and language branches of the CLIP model to improve alignment between the vision and language representations. Different from other methods that appends trainable prompts in the word embedding space, the prompts in MaPLe are appended to deep features of the image encoder and the text encoder. By modeling the stage-wise feature relationships progressively, MaPLe enables richer contexts and establishes state-of-the-art performance on several benchmarks.

## D. Details of the Three CAT Variants

In this work, we conquer the BNT problem by simultaneously preserving base-specific and task-shared knowledge in feature channels during prompt tuning. To achieve this goal, we devise the Channel Adjusted Transfer (CAT) head, which consists of two independent channel-wise Transformation (cwT) layers to transform image and text features to a new feature space, together with a linear classifier to promote the learning of base-specific knowledge in the transformed feature space. We illustrate the devised CAT head as well as its three variants in Figure 7, where we replace the two independent cwT layers (one for each modality) with a shared cwT layer in *v1*, we replace the linear classifier with

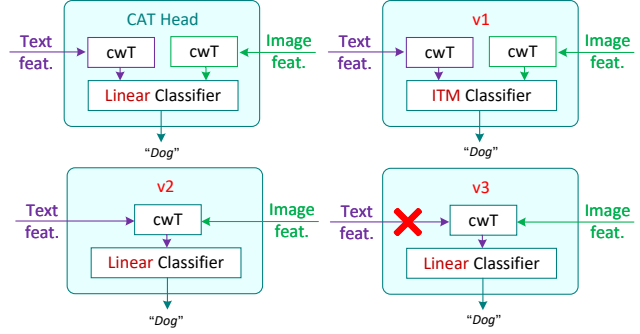


Figure 7. Illustration of three different variants (i.e., *v1*, *v2*, *v3*) of the developed CAT head in DePT.

an ITM classifier in *v2*, and we only feed image features to the liner classifier in *v3*. Experimental results in Section 3.2 of the paper demonstrate that the devised CAT head outperforms all the three variants.

## E. Performance of DePT under Different Shots

In our experiments, we follow CoOp [44], CoCoOp [43], KgCoOp [37] and MaPLe [19] to evaluate the generalization performance of models on many-way 16-shot base tasks – for every base task, 16 training examples are sampled from each class for prompt tuning. It is interesting to further scrutinize the effectiveness of our DePT in improving those baselines under different shots. Table 6 shows the base-to-new generalization performance of the four baselines w/ or w/o our DePT under different shots, where the reported results are the average of 11 datasets. As can be seen from the table, our DePT maintains the advantages across all 4-shot, 8-shot and 16-shot settings. Specifically, our DePT improve the performance of the baseline methods on both base and new tasks in almost all cases.

<sup>4</sup><https://github.com/htyao89/KgCoOp>

<sup>5</sup><https://github.com/muzairkhattak/multimodal-prompt-learning>



Method	4-Shot			8-Shot			16-Shot		
	Base	New	H	Base	New	H	Base	New	H
CoOp [44]	77.30	70.95	73.70	78.83	70.25	73.93	81.50	69.77	75.18
<b>+DePT</b>	<b>78.94</b>	<b>71.68</b>	<b>74.85</b>	<b>80.73</b>	<b>71.09</b>	<b>75.19</b>	<b>83.66</b>	<b>71.82</b>	<b>77.29</b>
CoCoOp [43]	76.56	<b>72.86</b>	74.66	78.57	72.40	75.36	81.18	72.18	76.42
<b>+DePT</b>	<b>78.77</b>	72.69	<b>75.61</b>	<b>81.12</b>	<b>72.43</b>	<b>76.53</b>	<b>83.80</b>	<b>72.89</b>	<b>77.97</b>
KgCoOp [37]	77.55	74.01	75.74	78.36	71.63	74.84	80.93	73.88	77.25
<b>+DePT</b>	<b>79.23</b>	<b>74.46</b>	<b>76.77</b>	<b>80.90</b>	<b>74.20</b>	<b>77.41</b>	<b>83.62</b>	<b>75.04</b>	<b>79.10</b>
MaPLe [19]	78.94	<b>73.63</b>	76.19	81.50	73.45	77.27	83.54	73.76	78.35
<b>+DePT</b>	<b>79.96</b>	73.50	<b>76.59</b>	<b>82.38</b>	<b>73.97</b>	<b>77.95</b>	<b>84.85</b>	<b>74.82</b>	<b>79.52</b>

Table 6. Base-to-new generalization performance of four baseline approaches w/ or w/o our DePT framework under different shots. The balance weight  $\lambda$  is fixed to 0.7 across all datasets and methods. The reported results are the average over 11 datasets.